On the Mechanism Behind the Instability of Isoreticular Metal-Organic Frameworks (IRMOFs) in Humid Environments

ARTICLE *in* CHEMISTRY - A EUROPEAN JOURNAL · SEPTEMBER 2012

Impact Factor: 5.73 · DOI: 10.1002/chem.201201212 · Source: PubMed

5 AUTHORS, INCLUDING:

Luca Bellarosa
ICIQ Institute of Chemical Research of Catal…
24 PUBLICATIONS **206** CITATIONS
SEE PROFILE

J. M. Castillo
Universidad Pablo de Olavide
21 PUBLICATIONS **435** CITATIONS
SEE PROFILE

Sofia Calero
Universidad Pablo de Olavide
164 PUBLICATIONS **2,782** CITATIONS
SEE PROFILE

Nuria López
ICIQ Institute of Chemical Research of Catal…
142 PUBLICATIONS **5,162** CITATIONS
SEE PROFILE

CHEMISTRY
A EUROPEAN JOURNAL

ChemPubSoc
Europe

DOI: 10.1002/chem.201201212

On the Mechanism Behind the Instability of Isoreticular Metal–Organic Frameworks (IRMOFs) in Humid Environments

Luca Bellarosa,[a] Juan Manuel Castillo,[b] Thijs Vlugt,[c] Sofía Calero,*[b] and Núria López*[a]

Abstract: Increasing the resistance to humid environments is mandatory for the implementation of isoreticular metal–organic frameworks (IRMOFs) in industry. To date, the causes behind the sensitivity of $[Zn_4(\mu_4\text{-}O)(\mu\text{-}bdc)_3]_8$ (IRMOF-1; bdc = 1,4-benzenedicarboxylate) to water remain still open. A multiscale scheme that combines Monte Carlo simulations, density functional theory and first-principles Born–Oppenheimer molecular dynamics on IRMOF-1 was employed to unravel the underlying atomistic mechanism responsible for lattice disruption. At very low water contents, H_2O molecules are isolated in the lattice but provoke a dynamic opening of the terephthalic acid, and the lattice collapse occurs at about 6% water weight at room temperature. The ability of Zn to form fivefold coordination spheres and the increasing basicity of water when forming clusters are responsible for the displacement of the organic linker. The present results pave the way for synthetic challenges with new target linkers that might provide more robust IRMOF structures.

Keywords: metal–organic frameworks · molecular dynamics · Monte Carlo simulations · multiscale modeling · water chemistry

Introduction

Metal–organic frameworks (MOFs)[1] are a relatively new class of hybrid materials that are characterised by secondary inorganic building units (SBUs) linked by organic structures that form three-dimensional periodic networks.[2] SBUs determine the symmetry of the lattice and give rise to a plethora of structures with desirable pore sizes and surface areas (up to $6000\ m^2g^{-1}$).[3–9] It is even possible to modify the organic units by including side chains with different functionalities,[10] which add a new level of complexity to the materials. These properties make MOFs promising materials in industry for gas purification,[11] separation,[12–16] storage[17–19] and heterogeneous catalysis.[20–24] However, their commercial implementation depends on the stability of these materials against the environment. One type of MOF, isoreticular MOF (or IRMOF), has a relatively high thermal stability, but degrades easily in humid air at room temperature.[25–30] Modifications with Br or NH_2 to form IRMOF-2 or IRMOF-3 structures are known to be more robust[31] but this strategy usually reduces the surface area despite slightly raising humidity tolerance.[32] Other metal–organic frameworks that also contain Zn but with different ligands (imidazoles) have been recently found to be more water-resistant but present a completely different tridimensional structure.[33]

Understanding the underlying mechanism of IRMOF degradation is mandatory[34] to devise new synthetic targets with tailored properties that can foster crystal engineering. Experimentally, the analysis of the intermediates of the hydrolysis is not straightforward and thus theoretical simulations are essential. The first classical molecular dynamics (MD) simulations observed a $[Zn_4(\mu_4\text{-}O)(\mu\text{-}bdc)_3]_8$ (IRMOF-1; bdc = 1,4-benzenedicarboxylate) lattice collapse at 4% water weight due to the rupture of the bond between a Zn atom and the central O atom from the Zn_4O core.[34] Recent experiments indicate slightly higher water tolerance of about 4–8% water weight.[26] MD simulations with ReaxFF force field[35] suggest water dissociation and protonation of the carboxylate moiety with subsequent linker liberation. In contrast, static ab initio simulations on cluster models with a single water molecule point out that the first broken bond is that of Zn to the terephthalic linker.[36] However, these theoretical approaches are not conclusive on the bond-breaking pattern or on the degree of water tolerance. Moreover, only few of these techniques can simultaneously provide an accurate description of bond formation, breaking and changes in coordination numbers (which are lacking in classical MD), and this only after a judicious fit against proper training set,

[a] Dr. L. Bellarosa, Prof. N. López
Institute of Chemical Research of Catalonia, ICIQ
Av. Països Catalans 16, 43007, Tarragona (Spain)
Fax: (+34) 977-920-231
E-mail: nlopez@iciq.es

[b] Dr. J. M. Castillo, Dr. S. Calero
Department of Chemical and Natural Systems
University Pablo de Olavide
Ctra. De Utrera km. 1, 41013 Seville (Spain)

[c] Prof. T. J. H. Vlugt
Process and Energy Laboratory
Leeghwaterstraat 44
2628 CA Delft (The Netherlands)

Supporting information for this article is available on the WWW under http://dx.doi.org/10.1002/chem.201201212.

thus limiting the transferability of the methodology. As far as the cluster models are concerned, they fail by construction to describe the lattice stiffness of the model, as well as the cooperative and dynamic effects of water.[37]

A proper study of the IRMOF-1 lattice stability under humidity calls for the use of multiscale methods that describe configurational contributions while keeping an atomistic and dynamic perspective. In our approach, water distributions were obtained from Monte Carlo simulations for which detailed electronic structure calculations on the basis of density functional theory (DFT) and massively parallel first-principles Born–Oppenheimer molecular dynamic (BOMD) simulations were carried out (Figure 1). The computationally very demanding BOMD can simultaneously resolve the electronic and ionic movements with the final goal of accounting for the dynamics and collective effects of water molecules.

Results and Discussion

Monte Carlo simulations: The Monte Carlo simulations show that isolated water molecules sit close to the Zn atoms (see Figure 2, inset 1). More generally, if few water molecules are added to the MC simulation box, they tend to disperse among all the possible unoccupied Zn centres in the lattice (Figure 2, insets 2 and 4), and when absorbed at the same Zn_4O core, water molecules tend to distribute around the vicinity of different Zn atoms as shown in Figure 2, inset 3. Water only agglomerates on a given IRMOF-1 pocket when many of the possible Zn_4O sites are already covered; this corresponds to six water molecules per MC simulation box (1.8% weight). Water trimers, tetramers and pentamers are sometimes seen at contents lower than 4% weight. If the starting configuration in the MC simulations shows two preabsorbed water molecules at the same Zn atom, the incoming water molecule has a very strong preference to form a water trimer as shown in Figure 2, inset 3.

Model systems with density functional theory: The Monte Carlo model system corresponds to the cell of stoichiometry $[Zn_4(\mu_4\text{-}O)(\mu\text{-}bdc)_3]_8$ of 424 atoms in which all the terephthalic units are planar. Because this system is too large for massive electronic structure calculations (especially BOMD ones), we have performed tests to construct a suitable model. Starting from the cubic crystallographic cell (MC cell), it is possible to construct a smaller lattice that makes both the calculations possible and the analysis simpler. This simplification leads to a model of $[Zn_4(\mu_4\text{-}O)(\mu\text{-}bdc)_3]$ (53-atom cell) stoichiometry (see Figure 1) in which a slight twist of the terephthalic linkers has been enforced. Thus the model corresponds to one-eighth of the initial cell. To analyse the relative energy of the high-energy constructed polymorph, we have tested two different properties. For instance, the formation energy according to the reaction $4\,ZnO(crystal) + 3\,H_2bdc \rightarrow Zn_4O(bdc)_3 + 3\,H_2O$ of the MC cell at the DFT level is found to be −0.50 eV per Zn atom and the cell parameter is 25.832 Å. The small DFT model provides instead −0.41 eV per Zn atom and 12.916 Å (which corresponds to 25.832 Å for the large cubic cell). Finally, the experimental results are 25.669 Å for the cell parameter,[1] and for the formation energy in *N*,*N*-diethylformamide (DEF), the formation is −0.26 eV per Zn.[38] Therefore, both the geometric and energy results of the high-energy isomer simulated in the DFT model system are in the same range as the error caused by the use of the functional.

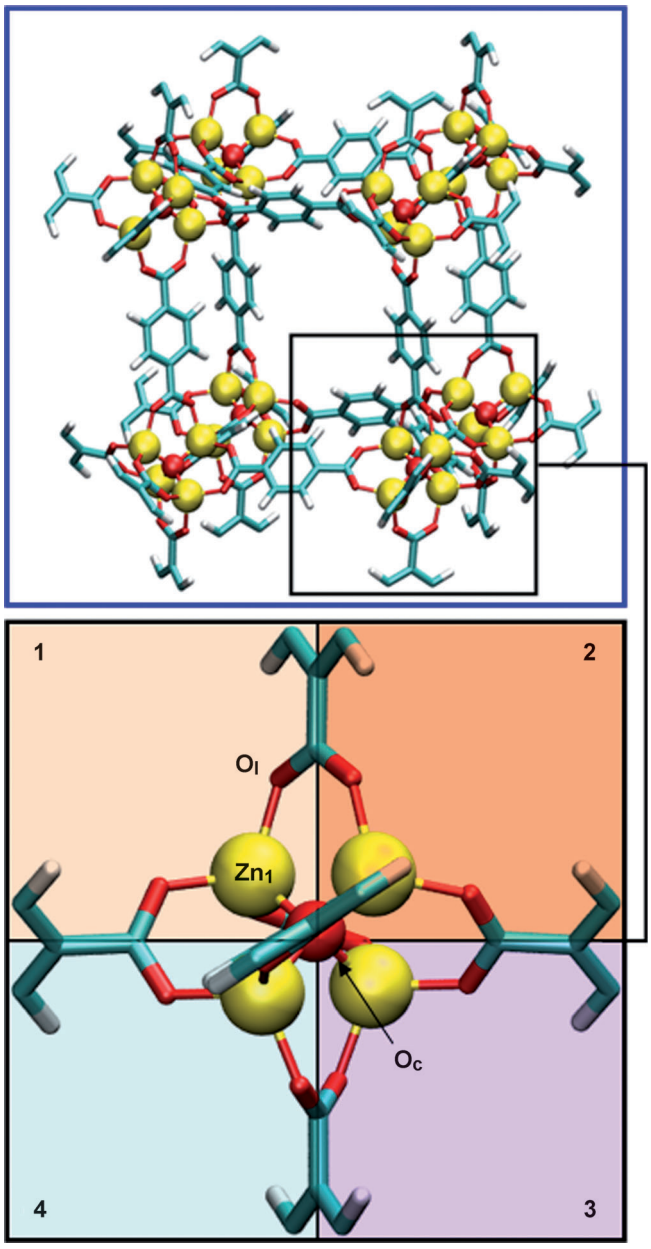

Figure 1. Projection of the Monte Carlo simulation box (blue square, stoichiometry $[Zn_4(\mu_4\text{-}O)(\mu\text{-}bdc)_3]_8$ 424 atoms) and DFT model system (black square, stoichiometry $[Zn_4(\mu_4\text{-}O)(\mu\text{-}bdc)_3]$ 53 atoms) for the IRMOF-1 lattice. Each Zn atom is placed at the centre of a tetrahedron formed by 4 oxygen atoms: three belong to the dibenzocarboxylic acids, O_l, and there is the central oxygen, O_c. The four quadrants (or pockets) are numbered in the black inset.

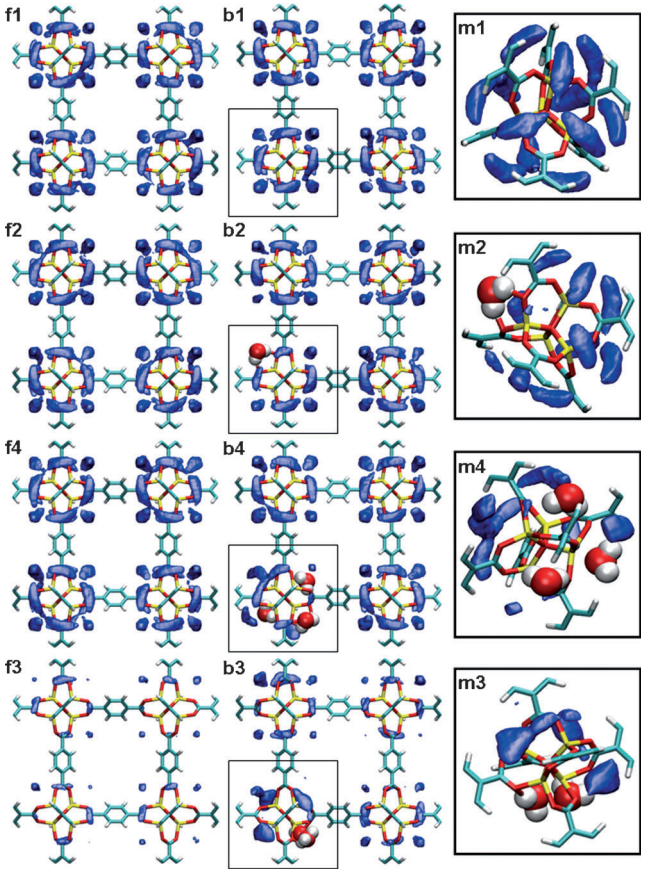

Figure 2. Probability for water absorption as obtained from MC simulations for the IRMOF-1 supercell $[Zn_4(\mu_4\text{-}O)(\mu\text{-}bdc)_3]_8$ at different water contents. Three different perspectives are shown: front (F) and back (B) views and unit cell detail (M) marked in black. The numbers indicate the total amount of water molecules in the simulation box. The results shown here correspond to a system with initially zero (F1, B1 and M1), one (F2, B2 and M2) and three initial water molecules (F4, B4 and M4) preabsorbed at different Zn atoms of the same unit cell, and two water molecules sitting at the same Zn centre (F3, B3 and M3). Preabsorbed water molecules are represented by spheres.

verts[42] the stability ordering and thus both the DFT and the MC models are consistent and provide the same ground state at this temperature: a water molecule coordinated to Zn and a free water molecule. Minimisations for the IRMOF-1 lattice that contains three and four water molecules result in two kinds of structures that show either isolated molecules in different Zn pockets (compatible with the MC minima in Figure 2) or chains and clusters on the same Zn centre. In the case of five water molecules, the formation of chains is unavoidable and, upon optimisation, two of the structures have one of the Zn–O_l bonds broken.

Again, we have assessed the properties of the DFT model with respect to that of the MC structure for the absorption of water clusters in the structure. Results are reported in Table 1. All the fully relaxed anhydrous cells are character-

Table 1. Water-interaction energies, ΔE (in eV per water molecule), for the reaction $[Zn_4(\mu_4\text{-}O)(\mu\text{-}bdc)_3]_x + NH_2O \rightarrow [Zn_4(\mu_4\text{-}O)(\mu\text{-}bdc)_3]_x(H_2O)_N$, with $N=$ 1, 3 or 5 water molecules adsorbed onto a single Zn centre and the 53-atom ($x=1$) or 424-atom cell ($x=8$). For each geometry, the average Zn–O distances to the most relevant Zn centre are reported in Å.

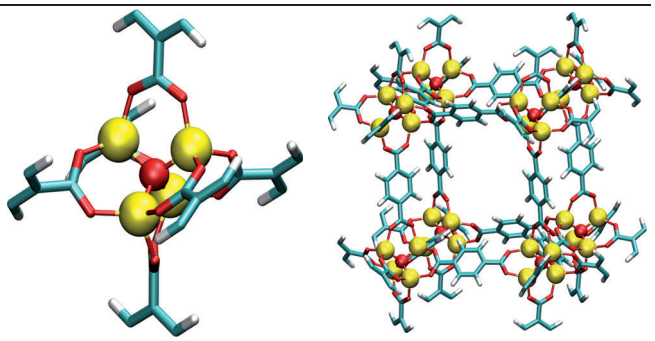

N	ΔE	d(Zn–O)	ΔE	d(Zn–O)
1	−0.21	2.070	−0.20	2.077
3	−0.30	2.079	−0.34	2.079
5	−0.37	2.062	−0.32	2.064

Once the small model was built, we optimised the structures at the DFT level for one to five water molecules (2.3–10.5%) in the DFT simulation box. For an isolated water molecule, two different local configurations compatible with the adsorption site detected in MC (Figure 2, inset 1) were identified with DFT: 1) close to the Zn site (fivefold Zn coordination, as for Zn^{2+} ions in water[39,40]); or 2) close to the linker O_l. Both structures are within 0.01 eV.

For two water molecules, the four initial structures compatible with the MC description yield H_2O molecules scattered on different Zn pockets. An alternative structure, which initially consisted of a water dimer close to one of the pockets, leads to a configuration in which the two water molecules interact with the same Zn. In fact, except for a similar configuration that had been previously reported by diffraction in the literature,[41] this structure is the most stable in the potential-energy surface by 0.32 eV. However, the introduction of entropic contributions at $T=300$ K reised by similar geometries around the Zn centres (average Zn–O distances are within 0.003 Å). When water is added to the system, the distortions of the metal centres are still quantitatively comparable, with a maximum discrepancy of 0.012 Å. In all studied cases, the average adsorption energy is within 0.1 eV, and is thus smaller than the entropic contribution for water in the gas phase at this temperature of 0.6 eV per water molecule, which indicates the predominance of entropic effects in the system and the robustness of the simplified DFT model.

The DFT optimisations presented here are not exhaustive because a huge number of low-energy geometries appear. Still, they reveal some interesting trends: water chain formation stabilises the system, and searching for the global minimum in the potential-energy surface is equivalent to maximising the number of hydrogen bonds. Moreover, many minima are accessible at room temperature. Therefore, two opposed driving forces emerge: entropy tends to distribute

water molecules in the lattice evenly, whereas hydrogen bonds keep water molecules as clustered as possible. The way to address this problem is by using first-principles molecular dynamics.

Born–Oppenheimer molecular dynamics: Seven BOMD water simulations were run at 300 K. In set 1, five trajectories with one to five water molecules were simulated starting from the MC-derived structures, that is, structures with 0.00 eV energy in the Supporting Information (Table S1 in the Supporting Information). In all cases, these structures show low water-clustering degrees. The two runs in set 2 correspond to systems with two and three water molecules for which the absolute minima of the DFT-optimised structures are taken as the starting point. Thus the latter contain water clusters. The BOMD trajectories are presented in Movies M1–M7 in the Supporting Information. The distance between the Zn being attacked by water and the most representative oxygen atom of the linker is shown in Figure 3. In the upper panel, the most remarkable distances between Zn and O_l for set 1 are reported, and in the lower panel, the length Zn–O_l for set 2 is shown.

In BOMD simulations in set 1 with 1, 2 or 3 molecules (between 2.3 to 6.6% weight), neither geometry modifications nor water clustering occurs. In all these simulations, water de-coordinates from the Zn centres and spends a large amount of time in the empty central cavity of the cell. The first indication of lattice disruption appears when four water molecules are present (8.6% weight). At this water content, the IRMOF-1-water system is quite dynamic (see snapshots and Movie M4 in the Supporting Information). After a period in which Zn_1 is fivefold-coordinated (to the ligands, O_c and water), one of the carboxylates opens up and coordinates to Zn_2 (see the violet inset in Figure 3), thus leaving Zn_1 fourfold-coordinated. A hydrogen bond forms between the displaced carboxylate and the water and keeps the former close to Zn_1. After 1 ps, the carboxylate returns to its initial position and regenerates the initial fivefold coordination sphere for Zn_1, which proves that the system behaves reversibly. The Zn–O_l distance ranges between 1.797 and 3.260 Å. However, after 15 ps the stress on the carboxylate is strong enough to displace it far away until the end of the simulation (20 ps).

For five molecules (10.5% weight), water quickly forms chains that easily degrade the lattice structure, thus opening up Zn–O_l and re-coordinating the COO^- subunit to the second Zn_2, as shown in the sky blue inset of Figure 3. No water dissociation is observed during the BOMD dynamics. Moreover, the coordination of the central O_c atom is always retained, even when the tetrahedral Zn_4O structure is significantly distorted. Thus the linker is attacked and replaced, which establishes the breaking pattern for the IRMOF-1 compound. Four water molecules can be taken as maximum water tolerance at room temperature, because no healing occurs over the complete simulation time.

The BOMD simulations on set 2 describe less probable initial conformations that might account for the water inhomogeneities found in some MC simulations. The results are summed up in the lower panel of Figure 3. For the dimer water chain, carboxylate displacement is observed, but when the second water molecule decoordinates from the first and starts wandering, the initial lattice is recovered (Movie M6 in the Supporting Information). For the water cluster trimer (Movie M7 in the Supporting Information), the Zn–O_l bond breaks up early in the simulation (≈1 ps) and the initial structure is never formed again. Therefore local water trimers are able to promote lattice disruption. A final investigation on the MC cell with 40 water molecules (10.5% weight) with BOMD was performed for completeness. Although this run was in the equilibrating period, the energy

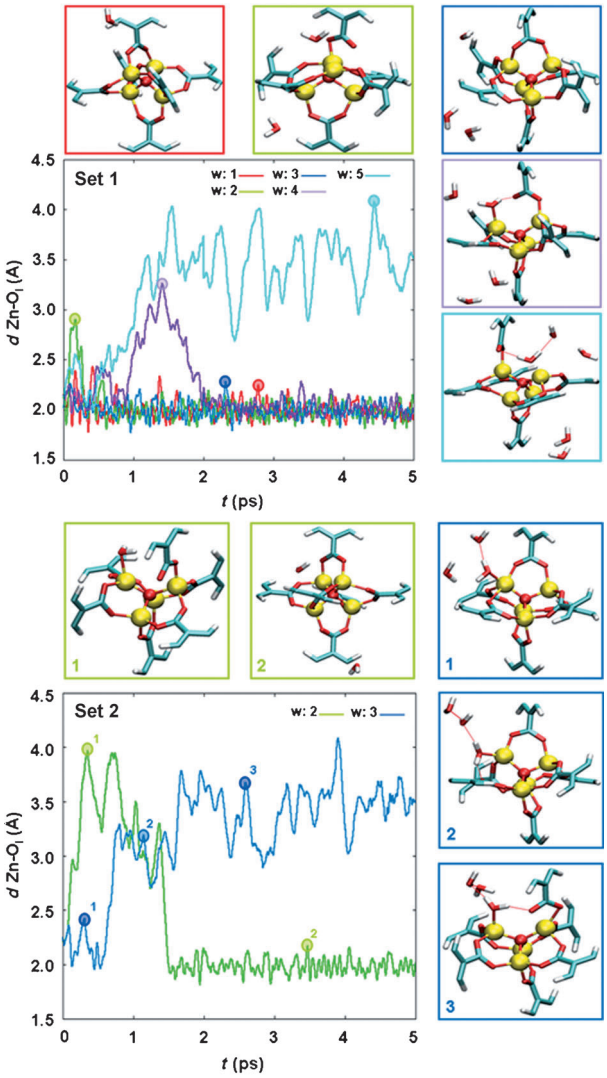

Figure 3. Relevant Zn–O_l distances, d(Zn–O_l), as a function of time for the BOMD in sets 1 and 2 with the number of water molecules per unit cell, w, together with key structures. The first 5 ps (2 of equilibration and 3 of simulation) are displayed. The BOMD trajectories are available in Movies M1–M7 in the Supporting Information. The insets describe the geometry of the system that corresponds to the position of the circle in the same colour. Upper panel: relevant distances for set 1; lower panel: relevant distances for set 2.

fluctuations after 0.05 ps are small (0.1–0.2 eV) and therefore similar to the oscillations found for the BOMD on the DFT model system. Therefore, a qualitative comparison between the reduced and the full-size models is possible. This run produces the same bond-breaking patterns as those found for the small cell with similar water content (Figure S4 in the Supporting Information). Thus, the water-tolerance threshold reported here is robust regardless of the size of the model.

For completeness we have also investigated the energy requirement for the protonation of the ligand to form the terephthalic acid that leaves a hydroxyl from water bonded to Zn. Starting by the initial configuration in Movie M7 in the Supporting Information (three water molecules) a potential-energy barrier of 0.77 eV is found (see Figure S6 in the Supporting Information for the reaction path). Although the barrier might seem achievable at room temperature, one ought to note that the initial configuration is very labile and will only be present for short times at medium water content. Thus, acid formation is an unlikely event under such conditions.

The reactivity found in the BOMD simulations can be understood by examining the basicity of the water molecules or clusters and comparing it to that of terephthalic acid. We have estimated basicity through the positions of the HOMO levels for the different water contents and configurations from the BOMD snapshots calculated from the isolated gas-phase molecules.[43] The HOMO of a single water molecule is more stable by almost 1 eV than that of the terephthalic ligand (see Figure 4), thus the former is less likely to share its density with the Zn^{2+} cations. The basicity is reversed for two interacting water molecules, and thus the water dimer can displace the linker. However, entropy does not favour dimer formation and, consequently, in dynamic simulations the dimer eventually separates. When the two water molecules stop interacting, the HOMO energy of the water plummets to that of the isolated water value. Then the linker can reform the broken bond, which leads to a complete recovery of the initial lattice structure. This mechanism is at the root of the reversibility found at low water contents. Increasing the number of water molecules further improves the basicity and reduces the entropic gains, and therefore ligand displacement is favourable.

Because water clustering is unavoidable, the best solution to improve the stability of the structure would be to find a linker that protects the Zn centres without compromising the pore size. To check this hypothesis, we have created a model system that is isostructural to IRMOF-1, in which all the oxygen atoms in the lattice have been substituted by sulfur atoms, S-IRMOF-1. This is a purely theoretical experiment, because there has been no success yet in the preparation of three-dimensional lattices with this particular ligand.[44] Therefore, although the synthesis might present hurdles, we consider this an interesting test of the methodology presented here. Indeed, BOMD simulations with five water molecules indicate that after the equilibration period the Zn–S bond is stable in the presence of the water cluster (see Figure 5 and Movies M8 and M9 in the Supporting Information). Therefore, the S-IRMOF is more robust than its oxygen counterpart, which indicates that it is possible to improve water tolerance of IRMOFs by a judicious choice of the ligand.

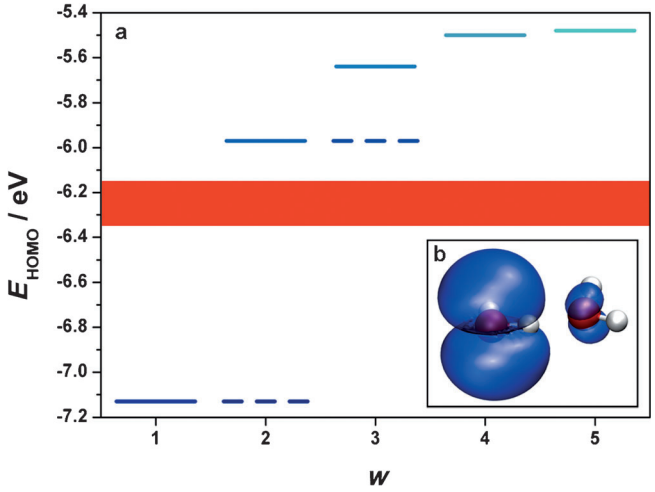

Figure 4. a) Solid lines represent the HOMO energy levels as a function of the number of water molecules, *w*, in the cluster. The red band represents the HOMO of terephthalic acid, including an error bar of 0.1 eV in the DFT (PBE) functional. The dotted lines represent the HOMO energies for two isolated water molecules or for the trimer when one molecule is separated. b) Inset of the HOMO of a cluster of two water molecules.

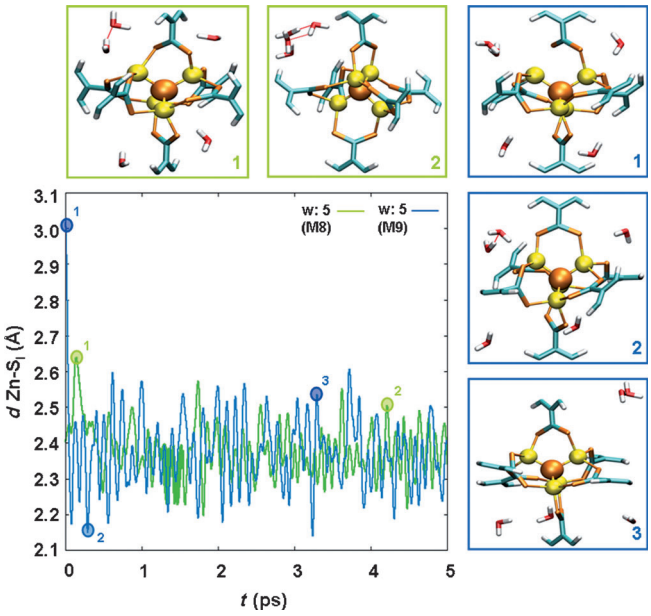

Figure 5. Relevant zinc–ligand, Zn–S_l, distances as a function of time [ps] for the BOMD trajectories with five water molecules. The first 5 ps (2 of equilibration and 3 of simulation) are displayed. The insets describe the geometry of the system that corresponds to the circles with the same colour and number. The BOMD trajectories are available in Movies M8 and M9 in the Supporting Information.

Conclusion

In summary, our multiscale theoretical study shows that the IRMOF-1 lattice disruption in humid ambient atmosphere occurs by the replacement of the terephthalic ligand by an intact water molecule, provided that the metallic centres of the structure are surrounded by small water aggregates. In the simulations we see that this takes place at about a 6% weight of water at 300 K, and it is mainly led by inhomogeneities in the water distributions identified in the MC simulations. On the basis of the DFT and BOMD simulations, the bond-breaking pattern does not involve the Zn bond with central oxygen or water dissociation. More importantly, the ability of Zn to form fivefold coordination spheres with the water molecules and the oxygen-containing ligands and the collective effects in water are crucial to understanding the linker stability under humid conditions. Since it is impossible to avoid formation of water chains or clusters, the synthetic strategy is to strengthen the Zn–ligand bonds through a proper selection of the linkers or by avoiding pentacoordinate structures with water as ligand.

The present multiscale methodology paves the way for the design of new compounds with targeted properties by indicating the role of the different actors in the lattice collapse under humid environments. Several computational techniques are needed to provide an accurate perspective at different scales: configurational considerations, detailed electronic structure and collective dynamics. Information descriptors, such as the HOMO position, inferred from our study can aid in the search for new materials. New synthetic challenges and opportunities naturally follow from the present methodology that might promote successful commercial applications of IRMOF materials.

Computational Methods

IRMOF-1, $[Zn_4(\mu_4\text{-}O)(\mu\text{-}bdc)_3]_8$, has a simple cubic arrangement of $(Zn_4O)(O_2C)_6$ octahedral cores linked by the benzene rings of 1,4-benzenedicarboxylate (see Figure 1). The most likely location of absorbed water molecules in the lattice was obtained by MC simulations in the NVT ensemble[45] for the lattice indicated by the blue square (top) in Figure 1 and at 300 K with an increasing number of molecules. MC simulations were performed in cycles, with twenty MC moves per cycle.

Every move consisted of translation, rotation or reinsertion of molecules, selected at random with equal probability. The maximum translational and rotational displacements were adjusted during the simulation to achieve an acceptance probability of 50%. The simulations were performed with an increasing number of water molecules at a fixed temperature of 300 K. In all cases, 5000 equilibration cycles and 2000000 production cycles were performed, analysing the positions of water molecules every 100 cycles. Water molecules were described using the Tip5pEw force field,[46] previously used to study the adsorption of water in MOFs.[47] More details on the simulation technique can be found elsewhere.[45,48–51] The system consisted of a IRMOF-1 cell of 25.832 Å (space group *Fm*3*m*), which was kept rigid during the simulation. The initial atomic positions of the MOF were taken from core–shell parameterisations, as well as the parameters for the dispersive interactions.[52] The force field consisted of dispersive interactions and Coulombic interactions. The former were modelled with Lennard–Jones potentials, truncated and shifted at a cutoff radius of 12 Å. Lorentz–Berthelot mixing rules were used to describe dispersive interactions between unlike atoms. Partial charges obtained by DFT simulations were placed at the position of the framework atoms as done in the literature[34] (see the Supporting Information). The Coulombic interactions were computed using the Ewald summation technique[53] with a relative accuracy of 10^{-6}. The simulations were performed by using a simulation package developed in our group. The parameters of the simulation are summarised in Table S4 of the Supporting Information.

DFT optimisations were performed on the IRMOF-1/water structures obtained by MC. With this purpose we employed the Vienna ab initio simulation package (VASP)[54,55] code with the PBE[56] functional. This functional provides a good balance in terms of accuracy and cost when water molecules/clusters are taken into account.[57,58] The inner electrons were replaced by PAW[59] (all-electron frozen core method) while the valence functions were expanded in plane waves with a cutoff energy of 400 eV and sampling was performed at the Γ point. The unit cell employed was simplified to an eighth of the MC cell (black square, Figure 1), considering only the octahedral secondary building unit and the six halves of the benzene rings, to allow the BOMD runs. This simplification of the model implies slight twists of the carboxylate units of the terephthalic linkers. The energy of this structure is only 0.09 eV per Zn atom higher than the crystallographic cell (see the Supporting Information). As the optimised cell for MC and DFT do not differ significantly (0.04 Å; see Table S1 in the Supporting Information) the DFT cell parameter was set to half of the MC value, 12.916 Å. The optimised cell was a cube of 14.206 Å for the sulfur IRMOF (S-IRMOF-1). Static calculations with between 1 and 5 water molecules were performed starting with MC and other different orientations to locate several minima for each system. For several of these structures, Born–Oppenheimer molecular dynamics simulations were performed with the same setup as described above, but with a cutoff energy of 500 eV to ensure a better convergence of the electronic density. The canonical ensemble (NVT) was employed at a temperature of 300 K, in which the temperature was controlled by using a Nosé thermostat, mass parameter 0.01 amu. For a proper description of the time evolution of the system, the convergence criterion in the electronic density of each minimisation was increased to 10^{-7} eV. This setup guaranteed proper energy conservation, that is, the drift of the expectation value of the extended system (ions + electrons + Nosé thermostat) is smaller than 0.002 eV ps^{-1} per unit cell. Initial equilibration steps were performed over 2 ps, whereas production runs were 20 ps long, and with a time step of 1 fs. Several tests that compared the MC and DFT models and the effect of different functionals and boundary conditions are presented in the Supporting Information and in reference 60.

Acknowledgements

We thank the MICINN projects CTQ2010-16077, CTQ2009-07753/BQU, CSD2006-0003, P07-FQM-02595, and ERC-Starting Grant Bio2chem-d for financial support and BSC-RES for providing generous computational resources. Prof. J. R. Galan-Mascarós is acknowledged for useful discussions.

[1] H. Li, M. Eddaoudi, M. O'Keeffe, O. M. Yaghi, *Nature* **1999**, *402*, 276–279.
[2] G. Férey, *Chem. Soc. Rev.* **2008**, *37*, 191–214.
[3] E. Y. Lee, M. P. Suh, *Angew. Chem.* **2004**, *116*, 2858–2861; *Angew. Chem. Int. Ed.* **2004**, *43*, 2798–2801.
[4] N. L. Rosi, J. Kim, M. Eddaoudi, B. L. Chen, M. O'Keeffe, O. M. Yaghi, *J. Am. Chem. Soc.* **2005**, *127*, 1504–1518.
[5] O. M. Yaghi, M. O'Keeffe, N. W. Ockwig, H. K. Chae, M. Eddaoudi, J. Kim, *Nature* **2003**, *423*, 705–714.
[6] X. B. Zhao, B. Xiao, A. J. Fletcher, K. M. Thomas, D. Bradshaw, M. J. Rosseinsky, *Science* **2004**, *306*, 1012–1015.
[7] G. Férey, C. Serre, *Chem. Soc. Rev.* **2009**, *38*, 1380–1399.

[8] H. X. Deng, C. J. Doonan, H. Furukawa, R. B. Ferreira, J. Towne, C. B. Knobler, B. Wang, O. M. Yaghi, *Science* **2010**, *327*, 846–850.
[9] O. M. Yaghi, Q. W. Li, *MRS Bull.* **2009**, *34*, 682–690.
[10] U. Mueller, M. Schubert, F. Teich, H. Puetter, K. Schierle-Arndt, J. Pastre, *J. Mater. Chem.* **2006**, *16*, 626–636.
[11] J. R. Li, R. J. Kuppler, H. C. Zhou, *Chem. Soc. Rev.* **2009**, *38*, 1477–1504.
[12] D. N. Dybtsev, H. Chun, S. H. Yoon, D. Kim, K. Kim, *J. Am. Chem. Soc.* **2004**, *126*, 32–33.
[13] L. Pan, D. H. Olson, L. R. Ciemnolonski, R. Heddy, J. Li, *Angew. Chem.* **2006**, *118*, 632–635; *Angew. Chem. Int. Ed.* **2006**, *45*, 616–619.
[14] R. Banerjee, A. Phan, B. Wang, C. Knobler, H. Furukawa, M. O'Keeffe, O. M. Yaghi, *Science* **2008**, *319*, 939–943.
[15] B. Wang, A. P. Cote, H. Furukawa, M. O'Keeffe, O. M. Yaghi, *Nature* **2008**, *453*, 207–211.
[16] L. J. Murray, M. Dinca, J. R. Long, *Chem. Soc. Rev.* **2009**, *38*, 1294–1314.
[17] S. S. Han, J. L. Mendoza-Cortes, W. A. Goddard, *Chem. Soc. Rev.* **2009**, *38*, 1460–1476.
[18] A. R. Millward, O. M. Yaghi, *J. Am. Chem. Soc.* **2005**, *127*, 17998–17999.
[19] R. Vaidhyanathan, D. Bradshaw, J. N. Rebilly, J. P. Barrio, J. A. Gould, N. G. Berry, M. J. Rosseinsky, *Angew. Chem.* **2006**, *118*, 6645–6649; *Angew. Chem. Int. Ed.* **2006**, *45*, 6495–6499.
[20] C. D. Wu, W. B. Lin, *Angew. Chem.* **2007**, *119*, 1093–1096; *Angew. Chem. Int. Ed.* **2007**, *46*, 1075–1078.
[21] S. H. Cho, B. Q. Ma, S. T. Nguyen, J. T. Hupp, T. E. Albrecht-Schmitt, *Chem. Commun.* **2006**, 2563–2565.
[22] J. Lee, O. K. Farha, J. Roberts, K. A. Scheidt, S. T. Nguyen, J. T. Hupp, *Chem. Soc. Rev.* **2009**, *38*, 1450–1459.
[23] A. U. Czaja, N. Trukhan, U. Muller, *Chem. Soc. Rev.* **2009**, *38*, 1284–1293.
[24] A. D. Burrows, K. Cassar, R. M. W. Friend, M. F. Mahon, S. P. Rigby, J. E. Warren, *CrystEngComm* **2005**, *7*, 548–550.
[25] S. S. Kaye, A. Dailly, O. M. Yaghi, J. R. Long, *J. Am. Chem. Soc.* **2007**, *129*, 14176–14177.
[26] L. M. Huang, H. T. Wang, J. X. Chen, Z. B. Wang, J. Y. Sun, D. Y. Zhao, Y. S. Yan, *Microporous Mesoporous Mater.* **2003**, *58*, 105–114.
[27] Y. Li, R. T. Yang, *Langmuir* **2007**, *23*, 12937–12944.
[28] S. Hausdorf, J. Wagler, R. Mossig, F. Mertens, *J. Phys. Chem. A* **2008**, *112*, 7567–7576.
[29] K. Schröck, F. Schroder, M. Heyden, R. A. Fischer, M. Havenith, *Phys. Chem. Chem. Phys.* **2008**, *10*, 4732–4739.
[30] J. G. Nguyen, S. M. Cohen, *J. Am. Chem. Soc.* **2010**, *132*, 4560–4561.
[31] M. Eddaoudi, J. Kim, N. Rosi, D. Vodak, J. Wachter, M. O'Keeffe, O. M. Yaghi, *Science* **2002**, *295*, 469–472.
[32] T. J. Wu, L. J. Shen, M. Luebbers, C. H. Hu, Q. M. Chen, Z. Ni, R. I. Masel, *Chem. Commun.* **2010**, *46*, 6120–6122.
[33] K. S. Park, Z. Ni, A. P. Cote, J. Y. Choi, R. D. Huang, F. J. Uribe-Romo, H. K. Chae, M. O'Keeffe, O. M. Yaghi, *Proc. Natl. Acad. Sci. USA* **2006**, *103*, 10186–10191.
[34] J. A. Greathouse, M. D. Allendorf, *J. Am. Chem. Soc.* **2006**, *128*, 10678–10679.
[35] S. S. Han, S. H. Choi, A. C. T. van Duin, *Chem. Commun.* **2010**, *46*, 5713–5715.
[36] J. J. Low, A. I. Benin, P. Jakubczak, J. F. Abrahamian, S. A. Faheem, R. R. Willis, *J. Am. Chem. Soc.* **2009**, *131*, 15834–15842.
[37] B. Guillot, *J. Mol. Liq.* **2002**, *101*, 219–260.
[38] J. T. Hughes, A. Navrotsky, *J. Am. Chem. Soc.* **2011**, *133*, 9184–9187.
[39] N. N. Greenwood, A. Earnshaw, *Chemistry of the Elements*, Elsevier, Burlington, **2002**.
[40] C. W. Bock, A. K. Katz, J. P. Glusker, *J. Am. Chem. Soc.* **1995**, *117*, 3754–3763.
[41] A. D. Burrows, C. G. Frost, M. F. Mahon, C. Richardson, *Angew. Chem.* **2008**, *120*, 8610–8614; *Angew. Chem. Int. Ed.* **2008**, *47*, 8482–8486.
[42] The molecular $T\Delta S$ contribution at 300 K for a water dimer is 0.33 eV, whereas the value for two isolated molecules is 0.76 eV.
[43] The HOMO energy levels were calculated for the isolated water clusters and terephthalic acid in a box of at least 12 Å sides at the Γ point.
[44] E. Neofotistou, C. D. Malliakas, P. N. Trikalitis, *Inorg. Chem.* **2007**, *46*, 8487–8489.
[45] D. Frenkel, B. Smit, *Understanding Molecular Simulation*, Academic Press, New York, **2002**.
[46] S. W. Rick, *J. Chem. Phys.* **2004**, *120*, 6085–6093.
[47] J. M. Castillo, T. J. H. Vlugt, S. Calero, *J. Phys. Chem. C* **2008**, *112*, 15934–15939.
[48] S. Calero, D. Dubbeldam, R. Krishna, B. Smit, T. J. H. Vlugt, J. F. M. Denayer, J. A. Martens, T. L. M. Maesen, *J. Am. Chem. Soc.* **2004**, *126*, 11377–11386.
[49] T. J. H. Vlugt, R. Krishna, B. Smit, *J. Phys. Chem. B* **1999**, *103*, 1102–1118.
[50] E. Jaramillo, M. Chandross, *J. Phys. Chem. B* **2004**, *108*, 20155–20159.
[51] D. Dubbeldam, S. Calero, T. J. H. Vlugt, R. Krishna, T. L. M. Maesen, E. Beerdsen, B. Smit, *Phys. Rev. Lett.* **2004**, *93*, 088302.
[52] D. Dubbeldam, K. S. Walton, D. E. Ellis, R. Q. Snurr, *Angew. Chem.* **2007**, *119*, 4580–4583; *Angew. Chem. Int. Ed.* **2007**, *46*, 4496–4499.
[53] P. P. Ewald, *Ann. Phys.* **1921**, *369*, 253–287.
[54] G. Kresse, J. Hafner, *Phys. Rev. B* **1993**, *47*, 558–561.
[55] G. Kresse, J. Furthmuller, *Phys. Rev. B* **1996**, *54*, 11169–11186.
[56] J. P. Perdew, K. Burke, M. Ernzerhof, *Phys. Rev. Lett.* **1996**, *77*, 3865–3868.
[57] J. Carrasco, A. Michaelides, M. Scheffler, *J. Chem. Phys.* **2009**, *130*, 184707.
[58] Tests on van der Waals contributions employing the D2 formulation (S. Grimme, *J. Comput. Chem.* **2006**, *27*, 1787) indicated larger interactions by about 0.10–0.15 eV. However, PBE+D2 resulted for different water configurations at constant water content showed energy differences (with respect to PBE) of about 0.01 eV per water molecule. See the Supporting Information for more details.
[59] P. E. Blöchl, *Phys. Rev. B* **1994**, *50*, 17953–17979.
[60] L. Bellarosa, S. Calero, N. López, *Phys. Chem. Chem. Phys.* **2012**, *14*, 7240–7245.

Received: April 10, 2012
Published online: August 21, 2012

